



ChemComm

Seeking a Au-C stretch on gold nanoparticles with ^{13}C -labeled N-heterocyclic carbenes

Journal:	<i>ChemComm</i>
Manuscript ID	CC-COM-10-2023-004973.R1
Article Type:	Communication

SCHOLARONE™
Manuscripts

COMMUNICATION

Seeking a Au-C stretch on gold nanoparticles with ^{13}C -labeled N-heterocyclic carbenes

Received 00th January 20xx,
Accepted 00th January 20xx

Isabel M. Jensen^{a,†}, Shayanta Chowdhury^{b,†}, Gaohe Hu^c, Lasse Jensen^{*,c}, Jon P. Camden^{*,b}, David M. Jenkins^{*,a}

DOI: 10.1039/x0xx00000x

Gold nanoparticles were functionalized with natural abundance and ^{13}C -labeled N-heterocyclic carbenes (NHCs) to investigate the Au-C stretch. A combinatorial approach of surface enhanced Raman spectroscopy (SERS) and density-functional theory (DFT) calculations highlighted vibrational modes significantly impacted by isotopic labeling at the carbene carbon. Critically, no isotopically-impacted stretching mode showed majority Au-C character.

Gold nanoparticles (AuNPs), long prized for their potential in biomedicine,^{1, 2} are rapidly emerging for orthogonal applications in sensing,³ catalysis,⁴ and photochemistry.⁵ Advances in these applications are accelerating due to development of N-heterocyclic carbenes as an innovative surface passivation substrate for gold surfaces.⁶⁻¹⁰ NHCs feature enhanced stability under a variety of thermal, chemical, and biological conditions compared to traditional surface ligands like thiols.^{11, 12} Given the myriad uses of NHC-functionalized gold nanoparticles, a fast and efficient method to determine chemisorption of the NHC to the AuNP is of paramount importance.

To date, the primary method to determine chemisorption of NHCs to AuNPs is X-ray photoelectron spectroscopy (XPS).^{11, 13-15} Chemisorption of NHCs on AuNPs is usually verified by the N 1s transition at 399.9-401.0 eV.^{7, 16, 17} Yet, there are two problems with XPS for fast, routine characterization of NHCs on

AuNPs. First, the signal for the N 1s transition is very weak. Second, the AuNP must be placed under high vacuum prior to measurement. A vibrational spectroscopic method, such as SERS, should allow for fast and effective determination of NHCs chemisorption under *in situ* or ambient conditions.

The significance of determining chemisorption of carbon ligands (derived from aryl diazonium salts) on gold nanoparticles led to competing SERS studies of functionalized AuNPs. McDermott and co-workers assigned the Au-C stretching mode to a low intensity band appearing at 412 cm^{-1} in the SERS spectrum by comparison with DFT calculations of a gold cluster.¹⁸ However, a recent SERS study with ^{13}C -labeled aryl diazoniums by Li and Plumeré revealed the assignment of the 412 cm^{-1} band may be erroneous, as their spectrum showed no shift of this peak with the ^{13}C isotope.¹⁹

Surface enhanced Raman spectroscopy of NHC-functionalized gold nanoparticles has rapidly developed since the discovery that gold complexes can be employed to append the NHCs to the AuNPs.^{6, 16, 20-23} Indeed, SERS measurements of NHCs on AuNPs have tracked post-synthetic modification on the nanoparticle surface²⁰ as well as monitoring ligand degradation in biological media.²¹ Yet, despite the proven utility of SERS for characterizing NHCs on AuNPs, no SERS study of the Au-C bond for NHCs on AuNPs has been conducted. The closest comparison is a tentative assignment of the Au-C bond stretch to 420 cm^{-1} on a Au(111) surface by Crudden and co-workers, who collected an HREELS spectra and simulated an IR spectra of a structurally similar, free gold complex.²⁴

To elucidate the Au-C stretching modes of a chemisorbed NHC, we synthesized the gold complex of the ^{13}C -carbene isotopologue of the diisopropyl benzimidazole NHC. This ^{13}C -labeled gold complex was appended to AuNPs and characterized by SERS, and there are clear distinctions in the spectra between the natural abundance and ^{13}C -labeled NHCs. DFT calculations for NHCs on gold clusters provide key insights into the modes that are isotopically impacted and reveal the

^a Department of Chemistry, The University of Tennessee, Knoxville, Tennessee 37996, United States.

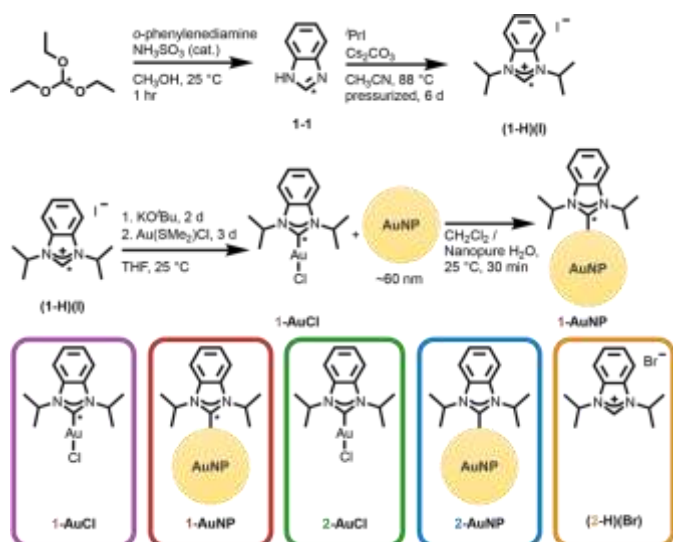
^b Department of Chemistry and Biochemistry, University of Notre Dame, Notre Dame, Indiana 46556, United States.

^c Department of Chemistry, The Pennsylvania State University, 104 Chemistry Building, University Park, Pennsylvania 16802, United States.

† These authors contributed equally

* Corresponding authors

Electronic Supplementary Information (ESI) available: Complete experimental details for synthesis and characterization of compounds (including spectra) as well as experimental details for Raman, SERS, and theoretical calculations. . See DOI: 10.1039/x0xx00000x



Scheme 1. Synthesis of ^{13}C labelled NHC gold complex (**1-AuCl**) and functionalized gold nanoparticle (**1-AuNP**). All of the species investigated in this study, including the natural abundance species (**2-H**)(Br), **2-AuCl**, and **2-AuNP**, are shown above and labelled with the corresponding colour on all of their spectra.

absence of a primary Au-C stretch in favour of more complex conjugated modes.

Synthesis of the ^{13}C -labelled benzimidazole (**1-1**) and benzimidazolium salt (**1-H**)(I) proceeded via modified literature methods from commercially available ^{13}C -formyl labelled triethyl orthoformate in two steps (Scheme 1).²⁵ Synthesis of the gold complex (**1-AuCl**) is challenging, as a typical base used for these reactions,^{6, 20, 23} potassium hexamethyldisilazane, generated an undesirable side product containing hexamethyldisilazane that could not be separated from the gold complex. Screening of alternative bases led to selection of potassium *tert*-butoxide, which, while slower to deprotonate (**1-H**)(I), cleanly generates the free carbene in THF at room temperature over two days. The free carbene was reacted in THF with $\text{Au}(\text{SMe}_2)\text{Cl}$ over three days at room temperature to provide mono-NHC gold chloride complex (**1-AuCl**). **1-AuCl** was purified via multiple rounds of column chromatography with two different stationary phases to remove the bis-NHC gold chloride complex. This process gave **1-AuCl** in 36% isolated yield. This laborious process was chosen to eliminate the possibility of halide confusion (between Cl and I), which we have previously found when using more conventional synthetic methods.²⁰ The enhanced carbene resonance from the ^{13}C -label is found in ^{13}C NMR at 176.33 ppm (Fig. S2). The isostructural unlabelled compounds **2-AuCl** and (**2-H**)(Br) were purchased from commercial vendors.

Both gold complexes, **1-AuCl** and **2-AuCl**, were separately appended to 60 nm quasi-spherical citrate-capped gold nanoparticles (AuNPs). The complexes were dissolved in solutions of methylene chloride and were then added to the nanoparticles in water at room temperature following our previously reported procedure, yielding the ^{13}C labelled **1-AuNP** and natural abundance **2-AuNP** from the corresponding complexes.²⁰ This method is known to form an Au-C bond between the NHC and the AuNP via an adatom.^{26, 27}

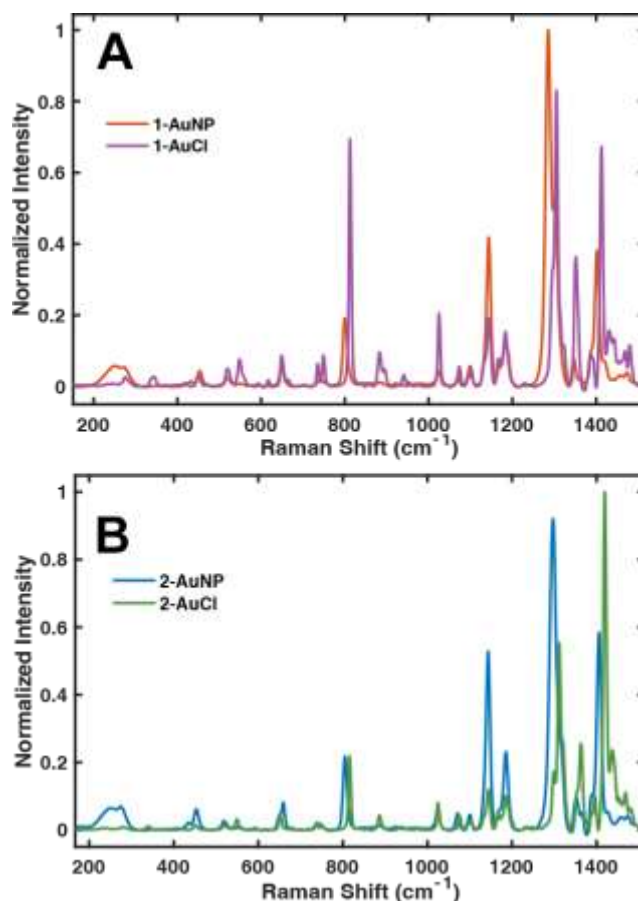


Fig 1. Direct comparisons of NHC-gold vibrational Raman and SERS spectra of gold complex and functionalized gold nanoparticles. **A.** ^{13}C labelled NHC as complex 1-AuCl and chemisorbed 1-AuNP. **B.** Natural abundance NHC as complex 2-AuCl and chemisorbed 2-AuNP.

We began by identifying the spectral differences between the chemisorbed and physisorbed NHCs. For the chemisorbed case, we employed **2-AuNP**. For the physisorbed case, we deposited the diisopropyl wingtip benzimidazolium bromide salt (**2-H**)(Br) (Scheme 1), which is unable to form a Au-C bond. The lack of Au-C bond for (**2-H**)(Br) is demonstrated by comparisons of both the SERS spectra (Fig. S5A) and the LDI-MS (Fig. S5B) versus **2-AuNP**.¹⁶ Of note is the appearance of a band at 423 cm^{-1} in the physisorbed case, which cannot be associated with a Au-C stretching mode as there is no Au-C bond present. The chemisorbed carbene from **2-AuNP** also displays peaks in this region, with a peak and shoulder appearing at 453 cm^{-1} and 430 cm^{-1} respectively.

A comparison of the vibrational spectra of the precursor NHC gold complexes versus the NHC-functionalized AuNPs is shown in Fig. 1. The evaluation of both spectra allowed us to identify four regions of interest: $425\text{-}435\text{ cm}^{-1}$, $650\text{-}660\text{ cm}^{-1}$, $795\text{-}805\text{ cm}^{-1}$, and $1285\text{-}1300\text{ cm}^{-1}$. In the SERS spectra for **1-AuNP**, a peak is observed at 430 cm^{-1} , but there is no corresponding peak in the Raman of **1-AuCl** (Fig. 1A). This distinction is what led McDermott to conclude this stretch is related to the Au-C bond in aryl films on gold nanoparticles.¹⁸

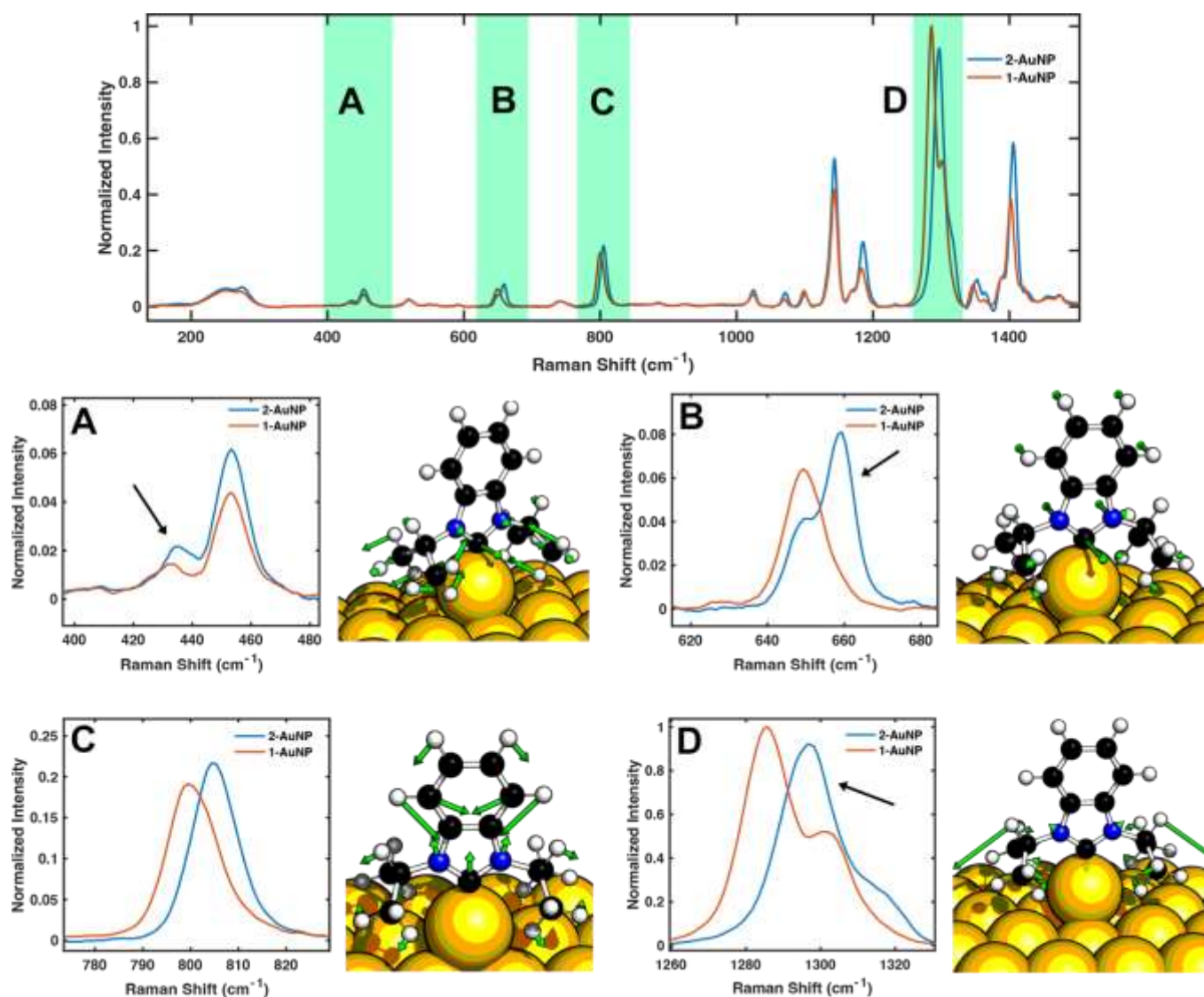


Fig. 2. Comparison of experimentally measured SERS vibrational spectra of ^{13}C -carbene labeled and natural abundance NHCs on gold nanoparticles, **1-AuNP** and **2-AuNP**, respectively. **Top:** Full range of relevant regions with highlighting (green) that show clear isotopic shifts. **A.** Close-up of 430/433 cm^{-1} peak and corresponding calculated vibrational mode. **B.** Close-up of 649/659 cm^{-1} peak and corresponding calculated vibrational mode. **C.** Close-up of 799/805 cm^{-1} peak and corresponding calculated vibrational mode. **D.** Close-up of 1286/1297 cm^{-1} peak and corresponding calculated vibrational mode.

In the 650 cm^{-1} region, we see a shift and the disappearance of a shouldering peak, most noticeable between **2-AuCl** and **2-AuNP** (Fig. 1B). The higher energy regions (around 800 cm^{-1} and 1300 cm^{-1}) both show a significant red shift between complex and nanoparticle.

A comparison of the surface-bound isotopically-labeled carbene versus natural abundance carbene shows significant shifts in these four regions of interest (Fig. 2). The SERS spectra shows red shifting in the **1-AuNP** spectra versus the **2-AuNP** spectra in four bands: 430 cm^{-1} /433 cm^{-1} , 649 cm^{-1} /659 cm^{-1} , 800 cm^{-1} /805 cm^{-1} , and 1286 cm^{-1} /1297 cm^{-1} . The more intense 450 cm^{-1} peak beside the faint 430 cm^{-1} peak did not shift at all between the isotopologues.

Computational modelling can assist in assigning the different modes in these four peaks that demonstrate isotopic

shifts. Computational Raman and SERS spectra for **1-AuNP**, **1-AuCl**, **2-AuNP** and **2-AuCl** were generated, and the corresponding peaks identified. The peak at 433 cm^{-1} correspond to the computational mode at 394 cm^{-1} , the peak at 659 cm^{-1} with a mode at 643 cm^{-1} , the peak at 805 cm^{-1} with a mode at 816 cm^{-1} , and the peak at 1297 cm^{-1} with a mode at 1272 cm^{-1} . The specific vibrational modes associated with each peak is shown in Fig. 2A-D. Further calculations to determine the weighted character of the vibrational modes found that the calculated peaks at 394 cm^{-1} and 643 cm^{-1} have around 33-37% carbene-carbon contribution to the vibrational mode, the calculated peak at 816 cm^{-1} has around 14% carbene carbon contribution, and the peak at 1272 cm^{-1} has 20% carbene carbon contribution. The two lower energy stretches have the carbon moving perpendicular to the Au-C bond, while the two

higher energy modes have the stretch in line with the Au-C bond. The combined results clearly indicate that the modes containing the carbene carbon contribution are quite complex, and the proposition of a localized Au-C stretch along the bond axis does not accurately represent the actual vibrational modes of the surface-bound NHC.

Taking all of the data together, we must conclude that for benzimidazolium-based NHCs on gold, there is no singular or distinct peak that can be considered a characteristic Au-C stretching mode on AuNPs. We believe that this result is due to the conjugation of the NHC ring system, which contributes to the overall delocalization of the normal modes over the entire molecule. Furthermore, we must caution against the use of low intensity bands near the 400-460 cm^{-1} region as diagnostic peaks for NHC chemisorption, as the normal modes for these NHCs are much too complex. Therefore, we believe that a more holistic evaluation of the entire vibrational spectra is necessary when confirming chemisorption of NHCs to gold nanoparticles.

Conflicts of interest

There are no conflicts of interest to declare.

Acknowledgements

We thank Nathaniel Dominique for LDI-MS data collection. This work was supported by the National Science Foundation under Grants CHE-2108328 (I.M.J. and D.M.J.), CHE-2108330 (S.C. and J.P.C.), and CHE-1856419 and CHE-2312222 (G.H. and L.J.). Any opinions, findings, and conclusions expressed in this material are those of the authors and do not necessarily reflect the views of the National Science Foundation.

References

1. S. A. Bansal, V. Kumar, J. Karimi, A. P. Singh and S. Kumar, *Nanoscale Advances*, 2020, **2**, 3764-3787.
2. K. Nejati, M. Dadashpour, T. Gharibi, H. Mellatyar and A. Akbarzadeh, *Journal of Cluster Science*, 2022, **33**, 1-16.
3. G. Zhang, *Nanotechnology Reviews*, 2013, **2**, 269-288.
4. M.-C. Daniel and D. Astruc, *Chemical Reviews*, 2004, **104**, 293-346.
5. H. Liang, Q. Chen, Q.-L. Mo, Y. Wu and F.-X. Xiao, *Journal of Materials Chemistry A*, 2023, **11**, 9401-9426.
6. N. L. Dominique, I. M. Jensen, G. Kaur, C. Q. Kotseos, W. C. Boggess, D. M. Jenkins and J. P. Camden, *Angewandte Chemie International Edition*, 2023, **62**, e202219182.
7. Y. Choi, C. S. Park, H.-V. Tran, C.-H. Li, C. M. Crudden and T. R. Lee, *ACS Applied Materials & Interfaces*, 2022, **14**, 44969-44980.
8. R. Ye, A. V. Zhukhovitskiy, R. V. Kazantsev, S. C. Fakra, B. B. Wickemeyer, F. D. Toste and G. A. Somorjai, *Journal of the American Chemical Society*, 2018, **140**, 4144-4149.
9. D. T. Nguyen, M. Freitag, C. Gutheil, K. Sotthewes, B. J. Tyler, M. Böckmann, M. Das, F. Schlüter, N. L. Doltsinis, H. F. Arlinghaus, B. J. Ravoo and F. Glorius, *Angewandte Chemie International Edition*, 2020, **59**, 13651-13656.
10. M. Koy, P. Bellotti, M. Das and F. Glorius, *Nature Catalysis*, 2021, **4**, 352-363.
11. G. Kaur, R. L. Thimes, J. P. Camden and D. M. Jenkins, *Chemical Communications*, 2022, **58**, 13188-13197.
12. C. A. Smith, M. R. Narouz, P. A. Lummis, I. Singh, A. Nazemi, C.-H. Li and C. M. Crudden, *Chemical Reviews*, 2019, **119**, 4986-5056.
13. N. Bridonneau, L. Hippolyte, D. Mercier, D. Portehault, M. Desage-El Murr, P. Marcus, L. Fensterbank, C. Chanéac and F. Ribot, *Dalton Transactions*, 2018, **47**, 6850-6859.
14. R. W. Y. Man, C.-H. Li, M. W. A. MacLean, O. V. Zenkina, M. T. Zamora, L. N. Saunders, A. Rousina-Webb, M. Nambo and C. M. Crudden, *Journal of the American Chemical Society*, 2018, **140**, 1576-1579.
15. Q. Wu, R. Peng, F. Gong, Y. Luo, H. Zhang and Q. Cui, *Colloids and Surfaces A: Physicochemical and Engineering Aspects*, 2022, **645**, 128934.
16. N. L. Dominique, R. Chen, A. V. B. Santos, S. L. Strausser, T. Rauch, C. Q. Kotseos, W. C. Boggess, L. Jensen, D. M. Jenkins and J. P. Camden, *Inorganic Chemistry Frontiers*, 2022, **9**, 6279-6287.
17. A. Inayeh, R. R. K. Groome, I. Singh, A. J. Veinot, F. C. de Lima, R. H. Miwa, C. M. Crudden and A. B. McLean, *Nature Communications*, 2021, **12**, 4034.
18. L. Laurentius, S. R. Stoyanov, S. Gusarov, A. Kovalenko, R. Du, G. P. Lopinski and M. T. McDermott, *ACS Nano*, 2011, **5**, 4219-4227.
19. H. Li, G. Kopiec, F. Müller, F. Nyßen, K. Shimizu, M. Ceccato, K. Daasbjerg and N. Plumeré, *JACS Au*, 2021, **1**, 362-368.
20. J. F. DeJesus, L. M. Sherman, D. J. Yohannan, J. C. Becca, S. L. Strausser, L. F. P. Karger, L. Jensen, D. M. Jenkins and J. P. Camden, *Angewandte Chemie International Edition*, 2020, **59**, 7585-7590.
21. L. M. Sherman, M. D. Finley, R. K. Borsari, N. Schuster-Little, S. L. Strausser, R. J. Whelan, D. M. Jenkins and J. P. Camden, *ACS Omega*, 2022, **7**, 1444-1451.
22. R. L. Thimes, A. V. B. Santos, R. Chen, G. Kaur, L. Jensen, D. M. Jenkins and J. P. Camden, *The Journal of Physical Chemistry Letters*, 2023, **14**, 4219-4224.
23. N. L. Dominique, S. L. Strausser, J. E. Olson, W. C. Boggess, D. M. Jenkins and J. P. Camden, *Analytical Chemistry*, 2021, **93**, 13534-13538.
24. C. M. Crudden, J. H. Horton, M. R. Narouz, Z. Li, C. A. Smith, K. Munro, C. J. Baddeley, C. R. Larrea, B. Drevniok, B. Thanabalasingam, A. B. McLean, O. V. Zenkina, I. I. Ebralidze, Z. She, H.-B. Kraatz, N. J. Mosey, L. N. Saunders and A. Yagi, *Nature Communications*, 2016, **7**, 12654.
25. Z.-H. Zhang, T.-S. Li and J.-J. Li, *Monatshefte für Chemie - Chemical Monthly*, 2007, **138**, 89-94.
26. M. J. Trujillo, S. L. Strausser, J. C. Becca, J. F. DeJesus, L. Jensen, D. M. Jenkins and J. P. Camden, *The Journal of Physical Chemistry Letters*, 2018, **9**, 6779-6785.
27. G. Wang, A. Rühling, S. Amirjalayer, M. Knor, J. B. Ernst, C. Richter, H.-J. Gao, A. Timmer, H.-Y. Gao, N. L. Doltsinis, F. Glorius and H. Fuchs, *Nature Chemistry*, 2017, **9**, 152-156.